A THOMAS-FERMI MODEL OF LOCALIZATION OF PROTON IMPURITIES IN NEUTRON MATTER*

By M. Kutschera

H. Niewodniczański Institute of Nuclear Physics, Cracow**

and W. Wójcik

Institute of Physics, Technical University, Cracow***

(Received March 21, 1990)

We show that the proton impurity in a neutron matter can create an inhomogeneity in density which acts as a potential well localizing the proton's wave function. At low densities this inhomogeneity is a neutron bulge, whereas at high densities a neutron deficiency (bubble) occurs. We calculate variationally the proton's energy using a Gaussian wave function. The neutron background is treated in a Thomas-Fermi approximation. The Skyrme interactions are used. We find that the localized proton has lower energy than the plane wave proton for densities below the lower critical density $n_l \cong 0.3n_0$, and above the upper critical density $n_u \cong 2.2n_0$, where $n_0 = 0.17$ fm^{-3}. We discuss some implications of the proton localization for magnetic properties of neutron matter containing a small admixture of protons.

PACS numbers: 21.65+f; 97.60.Jd

1. Introduction

The behaviour of proton impurities in a neutron matter has not been studied in a wide density range. This is an interesting nuclear physics problem which has also consequences for neutron star physics. Neutron matter containing a small admixture of protons is the material which forms the inner crust and the core of a neutron star [1]. A crucial question is whether the proton component remains a normal Fermi liquid down to very low proton concentrations, or whether it shows a more complex behaviour. As was shown in Ref. [2], magnetic properties of strongly asymmetric nuclear matter depend sensitively on the behaviour of the proton admixture.

In this paper we study the behaviour of proton impurities in a neutron matter. It is known that the proton chemical potential in pure neutron matter is negative as a result

* This work was supported in part by M. Skłodowska-Curie Foundation, grant F-071-P and by Polish Ministry of National Education.

** Address: Instytut Fizyki Jądrowej, Radzikowskiego 152, 31-342 Kraków, Poland.

*** Address: Instytut Fizyki, Politechnika Krakowska, Podchorążych 1, 30-084 Kraków, Poland.

of attractive proton-neutron interactions. More importantly, however, various parametrizations show that it decreases fast with increasing neutron matter density, reaching a minimum roughly at the saturation density. At higher densities the proton chemical potential increases and becomes positive at high enough densities (Fig. 4). This suggests that a uniform density neutron matter surrounding a proton might not be the lowest energy state. A single proton in neutron matter can lower its energy by inducing a density inhomogeneity around it. This density excess at densities below n_1, and density reduction for densities above n_u, make the proton chemical potential lower and also produce an effective potential well, which can influence the proton's wave function.

In order to judge if the nonuniform density configuration is of lower energy one has to account also for the positive contributions to the energy. These arise due to the local change of the neutron matter density, the gradient of the neutron density and the proton momentum.

The problem we consider in this paper is closely related to the question of the effective mass of a proton impurity in the neutron medium. Baym, Bethe and Pethick [3] argued in a qualitative discussion that the proton effective mass in a neutron matter should be considerably higher than the bare mass. This is due to the attractive proton-neutron interactions. For highly asymmetric nuclear matter, containing a proton fraction of the order of a few percent, the proton effective mass was calculated by Sjöberg [4], who found the proton effective mass to be smaller than the bare mass. Sjöberg [4] assumed the system to be a two-component Fermi liquid. If the arguments of Refs. [3] and [4] are correct, there should exist a critical proton fraction, above which the proton effective mass abruptly decreases to the values found by Sjöberg.

Calculations which we present in this paper show that the single proton wave functions in neutron matter containing a small proton fraction are of finite extension rather than being plane waves, at least at densities below n_1 and above n_u. This means that a single proton is localized. In terms of the Landau Fermi-liquid theory, localization of quasiparticles corresponds to a divergent effective mass [5]. Thus the calculations presented here support the conjecture of Ref. [3].

The paper is organized as follows: In the next Section we present basic formulae describing the energy of the proton impurity in neutron matter for localized and nonlocalized impurities. In Sect. 3 we describe the Hamiltonian used to calculate the properties of neutron matter and the proton chemical potential. The Thomas-Fermi energy density for neutrons is also considered in this Section. In Sect. 4 the energy of the localized proton is calculated variationally. The results of our calculations are discussed in Sect. 5. In the last Section we briefly show implications of the proton localization for magnetic properties of neutron matter containing a small proton fraction.

2. Proton impurities in neutron matter

Let us consider a neutron matter containing a small proton fraction x. Our aim is to compare energies of two phases: a normal phase (of uniform density) and a phase with localized protons. We will proceed in the spirit of the Wigner-Seitz approximation and

divide the system into cells, each of them enclosing a single proton. For simplicity the cells are assumed to be spherical. The volume of the cell is $V = 1/n_P$, where the proton density $n_P \cong x n_N$ for small x.

The normal phase is of uniform neutron density n_N and the neutron chemical potential is μ_N. In the uniform density configuration protons are not localized and their wave functions are plane waves. The energy of the cell, which is a sum of proton and neutron energies, reads

$$E_0 = V\varepsilon(n_N, n_P), \tag{1}$$

where $\varepsilon(n_N, n_P)$ is the energy density of the uniform phase. For small proton density, i.e. for low x, we can expand the energy density

$$\varepsilon(n_N, n_P) \cong \varepsilon(n_N, 0) + \mu_P(n_N, 0) n_P. \tag{2}$$

In the following we shall adopt abbreviations $\varepsilon(n_N) = \varepsilon(n_N, 0)$ for the energy density of pure neutron matter and $\mu_P(n_N) = \mu_P(n_N, 0)$ for the proton chemical potential in pure neutron matter. The energy of the cell is thus approximately

$$E_0 = \mu_P(n_N) + V\varepsilon(n_N). \tag{3}$$

Our aim is to compare the energy of the normal phase, where protons are nonlocalized, with the energy of a phase where protons are trapped into potential wells, corresponding to the nonuniform neutron density distribution, which most likely form a regular arrangement. We treat this proton "crystal" in the Wigner-Seitz approximation.

Let us consider a Wigner-Seitz cell with nonuniform neutron matter distribution $n(r)$ surrounding the proton whose wave function is Ψ_P. In the local density approximation one can identify the proton effective potential with the local proton chemical potential μ_P, as will be shown in the next Section. The proton's effective potential varies locally with neutron matter density $n(r)$. This results in a potential well $\mu_P(n(r))$ which affects the single proton wave function. The energy of the Wigner-Seitz cell E_L, is:

$$E_L = \int_V d^3r \Psi_P^*(r) \left[-\frac{\nabla^2}{2m_*} + \mu_P(n(r)) \right] \Psi_P(r) + \int_V d^3r \varepsilon(n(r)) + B_N \int_V d^3r (\vec{\nabla} n(r))^2. \tag{4}$$

The first term is the energy of the proton confined to an effective potential well $v_{eff}(r) = \mu_P(n(r))$. This is an attractive potential well. When the derivative of the proton chemical potential with respect to the neutron density is negative, $n(r)$ is assumed to have a maximum at the center $r = 0$. At high densities the derivative of the proton chemical potential becomes positive and in this case $n(r)$ is assumed to have a minimum at the center. This is shown schematically in Figs. 1a and 1b. $\Psi_P(r)$ is the localized proton wave function. In Figs. 2 and 3 we show schematically the proton's probability distribution $\Psi_P^*(r)\Psi_P(r)$, and the effective potential $v_{eff}(r) = \mu_P(n(r))$.

The two other terms in the Eq. (4) describe the contributions to the energy due to the local change of the neutron Fermi momentum and the gradient of the neutron distribution, respectively, in the Thomas-Fermi approximation. Here $\varepsilon(n(r))$ is the local neutron matter energy per unit volume. The parameter B_N is the curvature coefficient for pure neutron

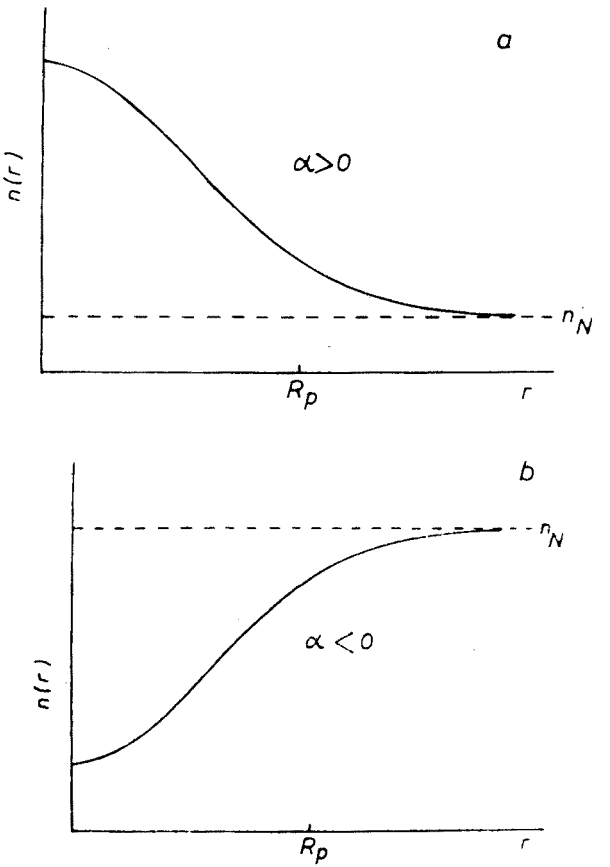

Fig. 1. The neutron density distribution in the Wigner-Seitz cell which lowers the proton's chemical potential for $n < n_1$ (a) and for $n > n_4$ (b)

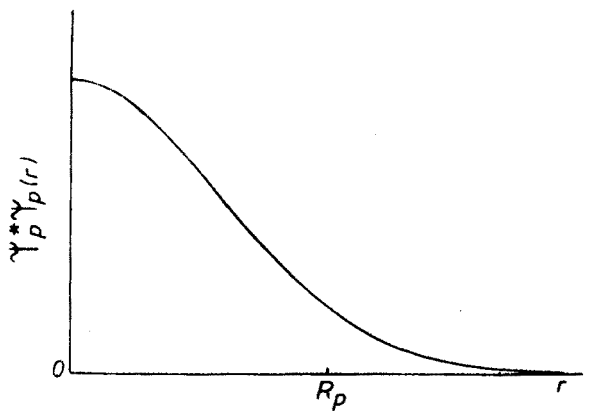

Fig. 2. The proton's probability distribution in the localized state

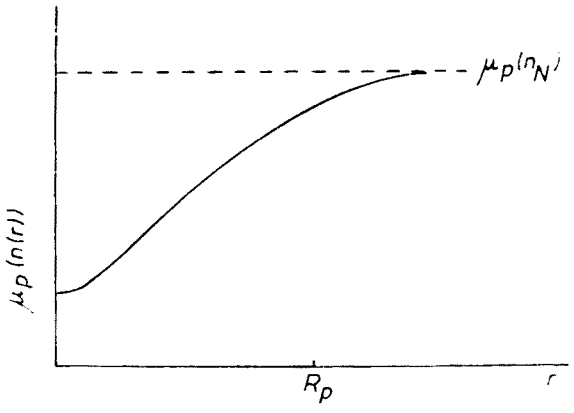

Fig. 3. The effective potential well corresponding to neutron density distributions of Fig. 1a and 1b. The localized proton is trapped into this potential well

matter. In Sect. 3 we describe the choice of B_N. The cell volume V in Eq. (4) is the same as in Eq. (3).

Let us remark that Eq. (4) has a typical form of the energy of non-topological solitons [6] for fermions interacting with background fields which form a bag-like configuration. In our case the neutron density $n(r)$ plays, in the Thomas-Fermi approximation, a role of the background field. The proton is confined to the "bag" made by the neutron density distribution.

To evaluate the energy E_L, Eq. (4), one can derive the Euler-Lagrange equations and solve them selfconsistently for $\Psi_p(r)$ and $n(r)$ with appropriate boundary conditions. If $E_L \leqslant E_0$, the localized proton wave function is the ground state of the system. In this paper we shall not attempt to find the minimum energy configurations by solving the full Euler-Lagrange equations. Instead we will use a variational ansatz for the proton wave function $\Psi_p(r)$ and for the neutron density distribution $n(r)$ containing variational parameters which will be optimized to give the minimum energy.

In order to decide which is the ground state configuration we should compare the energies E_0, Eq. (3), and E_L, Eq. (4), assuming the same number of neutrons:

$$\int_V d^3r n(r) = V n_N. \tag{5}$$

This means that the neutron density variation $\delta n(r) = n(r) - n_N$ conserves the baryon number:

$$\int_V d^3r \delta n(r) = 0. \tag{6}$$

Before evaluating the energy difference between the two configurations, $\Delta E = E_L - E_0$, we shall briefly describe the Hamiltonian we use.

3. The Hamiltonian

We choose to work with the Skyrme forces [13] to calculate the properties of the neutron matter and the proton chemical potential. The Skyrme forces were often used in studies of neutron star matter [7–10]. The Skyrme potential we use reads

$$v(\vec{r}) = t_0(1+x_0P_\sigma)\delta(\vec{r})+\tfrac{1}{2}\,t_1(\vec{k}'^2\delta(\vec{r})+\delta(\vec{r})\vec{k}^2)+t_2\vec{k}'\cdot\delta(\vec{r})\vec{k}$$
$$+\tfrac{1}{6}\,t_3(1+x_3P_\sigma)n^\gamma\delta(\vec{r}), \tag{7}$$

where $\vec{k} = i/2(\vec{\nabla}_1-\vec{\nabla}_2)$ acts on the right of the delta-function and $\vec{k}'$ is the same operator acting on the left of $\delta(\vec{r})$. P_σ is the spin exchange operator.

The Hartree-Fock Hamiltonian corresponding to the contact Skyrme potential (7) is of the form

$$H = \tfrac{1}{16}\,(3t_1-t_2)\,(\vec{\nabla}n_N+\vec{\nabla}n_P)^2-\tfrac{1}{32}\,(3t_1+t_2)\,(\vec{\nabla}n_N^2+\vec{\nabla}n_P^2)+H_1, \tag{8}$$

where H_1 reads

$$H_1 = \left(\frac{1}{2m_N}+B_N\right)\tau_N+\left(\frac{1}{2m_P}+B_P\right)\tau_P+n^2[b+dn^\gamma-(0.5-x)^2(a_3+a_4n^\gamma)], \tag{9}$$

with $b = 3t_0/8$, $d = t_3/16$, $a_3 = t_0(0.5+x_0)$ and $a_4 = t_3(0.5+x_3)/6$. Here τ_t and B_t are

$$\tau_t = \sum_i |\vec{\nabla}\phi_i^{(t)}|^2, \quad t = N, P, \tag{10}$$

$$B_t = \tfrac{1}{4}\,[(t_1+t_2)n+\tfrac{1}{2}\,n_t(t_2-t_1)], \quad t = N, P. \tag{11}$$

The proton fraction is x and the total density is $n = n_N+n_P$, where $n_t = \sum_i |\phi_i^{(t)}|^2$.

The Hartree-Fock Hamiltonian depends only on local densities of neutrons and protons, their gradients and on local kinetic energy densities for protons and neutrons. The latter quantities for plane waves become

$$\tau_t = \tfrac{3}{5}\,(3\pi^2)^{2/3}n_t^{5/3}, \quad t = N, P. \tag{12}$$

In our calculations we use two sets of the Skyrme force parameters. The first set, (I), is $t_0 = -1057.3$ MeV fm^3, $t_1 = 235.9$ MeV fm^5, $t_2 = -100.0$ MeV fm^5, $t_3 = 14463$ MeV fm^6, $x_0 = 0.2885$, $x_3 = 0.2257$ and $\gamma = 1.0$. These are the Vautherin and Brink [11] parameters modified as described in Ravenhall, Bennet and Pethick [12]. The second set (II) due to Lattimer [10] reads: $t_0 = -2499.85$ MeV fm^3, $t_1 = t_2 = 0.0$, $t_3 = 16410$ MeV fm$^{3+3\gamma}$, $x_0 = 0.2$, $x_3 = 0.1924$ and $\gamma = 0.209$.

3.1. Proton chemical potential in uniform neutron matter

The energy of the nonlocalized proton with the momentum $\vec{k}$ in a uniform density neutron matter is

$$E_P(\vec{k}) = \frac{\vec{k}^2}{2m_P}+\sum_{|\vec{l}|\leqslant k_F}\langle\vec{k},\vec{l}\,|v|\vec{k},\vec{l}\,\rangle, \tag{13}$$

where k_F is the neutron Fermi momentum. The proton chemical potential in this case is the energy (13) corresponding to zero momentum

$$\mu_P = E_P(\vec{k} = 0). \tag{14}$$

The proton energy $E_P(\vec{k})$, Eq. (13), for the potential (7) using Eq. (14) becomes

$$E_P(\vec{k}) = \frac{\vec{k}^2}{2m_P} + \tfrac{1}{4}(t_1 + t_2) n_N \vec{k}^2 + \mu_P(n_N). \tag{15}$$

We calculate the proton chemical potential using the Hamiltonian (9) since μ_P can be expressed as

$$\mu_P = \frac{\partial H_1}{\partial n_P}(n_N, n_P = 0). \tag{16}$$

This gives the proton chemical potential in the form

$$\mu_P = \tfrac{1}{4}\tau_N(t_1 + t_2) + 2n_N[b + dn_N^\gamma - \tfrac{1}{4}(a_3 + a_4 n_N^\gamma)]$$
$$+ n_N[d\gamma n_N^\gamma + a_3 + a_4(1 - \tfrac{1}{4}\gamma) n_N^\gamma]. \tag{17}$$

We show in Fig. 4 the proton chemical potential μ_P as a function of the neutron Fermi momentum k_F, for both sets of the Skyrme parameters. One can notice that μ_P decreases with increasing neutron Fermi momentum reaching a minimum at neutron densities close to the saturation density 0.17 fm^{-3}.

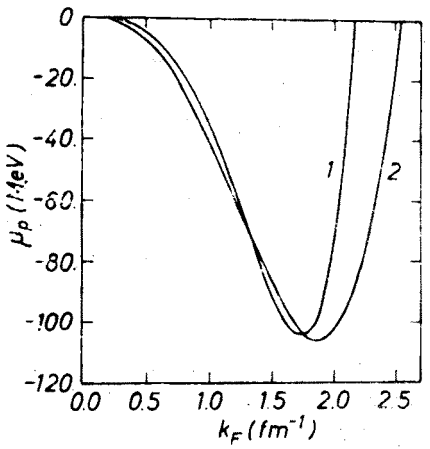

Fig. 4. The proton's chemical potential in pure neutron matter as a function of the neutron Fermi momentum k_F. The curves *1* and *2* correspond to the first (I) and second (II) set of the Skyrme force parameters, respectively

3.2. The proton effective potential in a local density approximation

Let us consider the energy of a single proton in a neutron matter of slightly nonuniform density $n(r)$. The proton will experience an effective potential associated with the neutron matter inhomogeneity and its wave function Ψ_P will no longer be a plane wave. The proton energy in a local density approximation becomes

$$E_P = \frac{1}{2m_P}\langle k\rangle^2 + \sum_{|\vec{l}|\leqslant k_F(r)} \langle \Psi_P, \vec{l}|v|\Psi_P, \vec{l}\rangle, \tag{18}$$

where $\langle k\rangle$ is the mean momentum of the proton, $k_F(r)$ is the local neutron Fermi momentum corresponding to the neutron density $n(r)$. Using Eq. (15) this formula gives

$$E_P = \int d^3r \left[\left[\frac{1}{2m_P} + \tfrac{1}{4}(t_1+t_2)n(r)\right]|\vec{\nabla}\Psi_P|^2 + \mu_P(n(r))\Psi_P^*\Psi_P\right]. \tag{19}$$

Expressing the proton energy in the form

$$E_P = \frac{1}{2m_*}\langle k\rangle^2 + \int d^3r \Psi_P^*(r) v_{\text{eff}}(r)\Psi_P(r) \tag{20}$$

we can identify the proton chemical potential $\mu_P(n(r))$ with the effective potential $v_{\text{eff}}(r)$.

The other terms in Eq. (19), the proton kinetic energy and the term representing the momentum dependence of the effective interaction, can be combined into a kinetic energy of the proton whose effective mass depends on local density:

$$\frac{1}{2m_*} = \frac{1}{2m_P} + \tfrac{1}{4}(t_1+t_2)n. \tag{21}$$

The second term here is proportional to the neutron matter density $n(r)$, therefore it is unimportant at low densities. At the saturation density this term for the first set of the Skyrme force parameters is a less than 30% correction to the kinetic energy. For the second set of the Skyrme parameters this term vanishes.

As we have explained, the density dependence of the proton effective mass is rather weak for densities below the saturation density and will be ignored in the following. At higher densities, $n > n_0$, the formula (21) will be used.

3.3. Thomas-Fermi energy of neutron matter

We will treat the neutron background in the Eq. (4) in the Thomas-Fermi approximation. This means that for the kinetic energy densities τ_t the formula (12) is used and an appropriate gradient term is introduced.

In the spirit of the nuclear Thomas-Fermi model [14–17] the energy of the neutrons in the cell can be written as

$$E_N = \int_V d^3r \varepsilon(n(r)) + B_N \int_V d^3r (\vec{\nabla} n(r))^2. \tag{22}$$

Here ε is the energy per unit volume in the local density approximation and we use the Hamiltonian H_1 (9) to obtain it.

The coefficient B_N of the gradient term in Eq. (4) is obtained as follows: In the nuclear Thomas-Fermi model the gradient term contribution to the energy density is

$$B_S[\vec{\nabla}(n_N+n_P)]^2, \tag{23}$$

with B_S obtained by fitting the properties of the nuclei. Conventionally B_S is written as

$$B_S = \frac{1}{8m}\eta \tag{24}$$

and $\eta = 12\,\mathrm{fm}^3$ gives the best agreement with the binding energies [15]. The surface thickness is however better reproduced for smaller values of η with $\eta \cong 8\,\mathrm{fm}^3$ giving the best values [15].

The coefficient B_S (24) is appropriate for symmetric nuclear systems with equal number of protons and neutrons. For isospin asymmetric systems a term of the form

$$-\frac{1}{8m}\vartheta[\vec{\nabla}(n_N-n_P)]^2 \tag{25}$$

should appear [3, 18, 19] in the energy density with $\vartheta \cong \eta/3$. Combining Eqs. (24) and (25) we find

$$B_N = \tfrac{2}{3}\frac{1}{8m}\eta. \tag{26}$$

In our numerical calculations we use $B_N = 31.6\,\mathrm{MeV\ fm}^5$ corresponding to $\eta \cong 9\,\mathrm{fm}^3$. Also $B_N = B_S$ for $\eta = 12\,\mathrm{fm}^3$ ($B_S = 62.2\,\mathrm{MeV\ fm}^5$) is used in order to show how the results depend on a particular choice of B_N. One can regard $B_S(\eta = 12\,\mathrm{fm}^3)$ as an upper limit of B_N.

4. Variational estimate of the energy of the localized proton

We assume a simple trial form of the proton wave function and the neutron density variation. For the proton wave function we use a Gaussian:

$$\Psi_P(r) = (\tfrac{2}{3}\pi R_P^2)^{-3/4}\exp\left(-\frac{3r^2}{4R_P^2}\right). \tag{27}$$

Here R_P is the rms radius of the localized proton probability distribution. We treat this quantity as a variational parameter and minimize ΔE with respect to R_P.

The neutron density variation $\delta n(r)$ is chosen to be:

$$\delta n(r) = \alpha\left(\Psi_P^*(r)\Psi_P(r) - \frac{1}{V}\right) \tag{28}$$

and the neutron density is

$$n(r) = n_N + \delta n(r). \tag{29}$$

Here α is the second variational parameter; $\alpha > 0$ corresponds to the neutron density enhancement around the proton and $\alpha < 0$ corresponds to the reduction of the neutron density in the proton vicinity as compared with the uniform background.

Using the trial forms of the proton wave function and the neutron density variation the energy difference ΔE becomes

$$\Delta E = \frac{9}{8m_*}\frac{1}{R_P^2} + \int_V d^3r \Psi_P^*(r)\,[\mu_P(n(r)) - \mu_P(n_N)]\Psi_P(r)$$

$$+ \int_V d^3r(\varepsilon(n(r)) - \varepsilon(n_N)) + B_N\alpha^2\,\tfrac{9}{2}\,(\tfrac{4}{3}\,\pi)^{-3/2}\,\frac{1}{R_P^5}\,. \tag{30}$$

The first term is the proton kinetic energy. The second term, which is attractive, originates from the interaction of the proton with the neutron background. The third term accounts for the local change of the neutron Fermi momentum. The last term is due to the gradient term in the Eq. (4). The gradient term plays a stabilizing role for small values of R_P.

We calculate the energy difference ΔE for small proton fraction x, i.e. in the limit of large volume V. The first and the last terms were calculated assuming that the Wigner-Seitz cell radius R_c is much bigger than R_P, $R_c \gg R_P$. Denoting $\Psi_P^*\Psi_P = p(r)$ and expanding in $1/V$ we have

$$\int d^3r\left[\mu_P\left(n_N + \alpha p - \alpha\frac{1}{V}\right) - \mu_P(n_N)\right]p = \int d^3r[\mu_P(n_N + \alpha p) - \mu_P(n_N)]p$$

$$-\alpha\frac{1}{V}\int d^3r\,\frac{\partial\mu_P}{\partial n}(n_N + \alpha p(r))p(r). \tag{31}$$

The integral in the second term does not depend on the cell volume so that this term vanishes in the limit $V \to \infty$. Expanding in the same way the energy density, we obtain from the third term in Eq. (30)

$$\int d^3r\left[\varepsilon\left(n_N + \alpha p - \alpha\frac{1}{V}\right) - \varepsilon(n_N)\right] = \int d^3r[\varepsilon(n_N + \alpha p) - \varepsilon(n_N)] - \alpha\mu_N(n_N)$$

$$-\alpha\frac{1}{V}\int d^3r[\mu_N(n_N + \alpha p) - \mu_N(n_N)]. \tag{32}$$

Here also the integral in the last term does not depend on the cell volume, since $p(r)$ is a Gaussian, and this term vanishes for large V.

The above procedure allowed us to separate contributions to ΔE which depend only on the neutron matter properties and the first order corrections in proton density n_p. These corrections play a crucial role in determining the critical proton fraction* x_c, above which a delocalization transition occurs.

The energy difference ΔE is shown schematically as a function of the proton localization radius R_p in Fig. 5. One can notice that there exists a range of values of R_p for which ΔE is negative. We denote by R_p^z the value of R_p corresponding to onset of instability, i.e. the highest value of R_p for which $\Delta E \leqslant 0$. R_p^m corresponds to the minimum of ΔE as a function of R_p and the value of ΔE at the minimum is ΔE_m.

In Fig. 6 we show the minimum energy difference ΔE_m as a function of the neutron

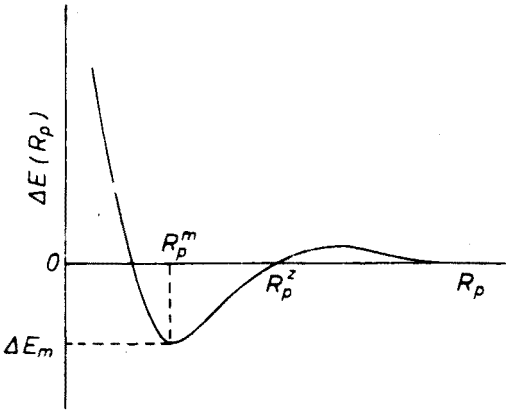

Fig. 5. The energy difference ΔE, Eq. (30), shown schematically as a function of the proton localization radius R_p for a fixed value of α. The minimum ΔE_m occurs at R_p^m. R_p^z corresponds to the onset of instability $\Delta E = 0$

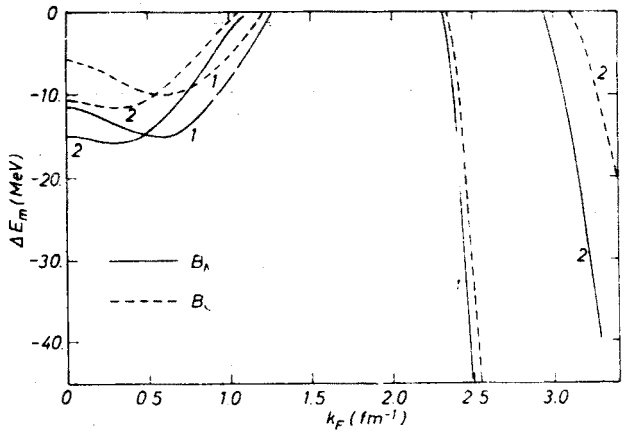

Fig. 6. The minimum energy difference ΔE_m, as defined in Fig. 5, as a function of the neutron Fermi momentum k_F. The curves *1* and *2* correspond to the first (I) and second (II) set of the Skyrme force parameters, respectively. Results for two values of the gradient term coefficient B_N are displayed

Fermi momentum for both sets of the Skyrme force parameters and for two values of the gradient term coefficient B_N. Only negative values are indicated. There are two distinct density regions where $\Delta E_m < 0$. For the first set of the Skyrme parameters and for the lower value of B_N these are densities below the lower critical density $n_l \cong 0.3n_0$ and above the upper critical density $n_u \cong 2.2n_0$. Negative values of ΔE indicate that the localized proton has lower energy than the proton whose wave function is a plane wave. The low--density localization corresponds to a local density enhancement around the proton ($\alpha = 2.0$), Fig. 1a. For densities above n_u, the proton is localized in a region of lower density as compared with the uniform background, i.e. there is a low-density bubble around the proton, Fig. 1b.

In Fig. 7 the radius R_p^z, below which the instability occurs, is displayed as a function of the neutron Fermi momentum for $\alpha = 2.0$ for densities $n < n_l$, and for $\alpha = -1.0$

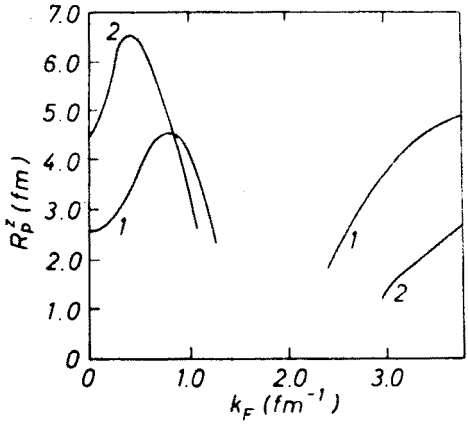

Fig. 7. The maximum localization radius R_p^z, as defined in Fig. 5, as a function of the neutron Fermi momentum k_F for the same sets of the Skyrme force parameters as in Figs. 4 and 6. The curves correspond to $B_N = 31.6$ MeV fm^5

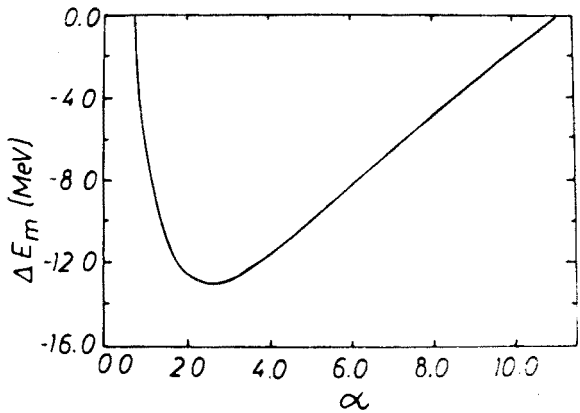

Fig. 8. The minimum energy difference ΔE_m as a function of the parameter α for density $n_N = 0.0185$ fm^{-3}

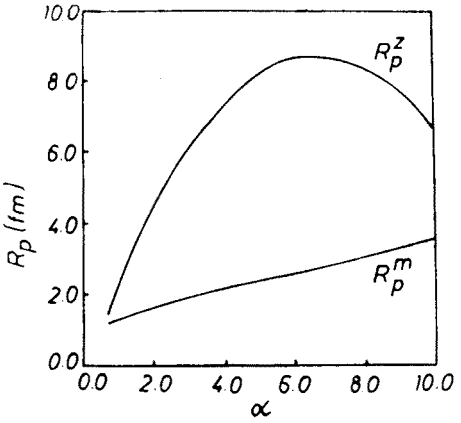

Fig. 9. The maximum localization radius R_P^z and the radius R_P^m corresponding to ΔE_m as functions of the parameter α for density $n_N = 0.0185\ \text{fm}^{-3}$

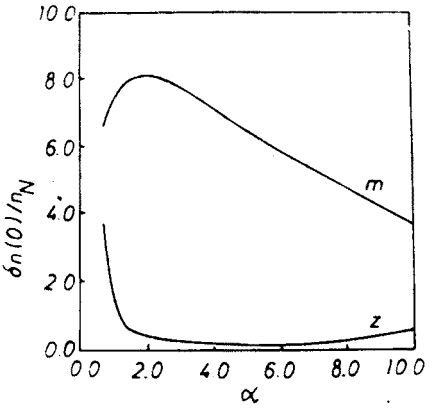

Fig. 10. The relative density excess at the center of the cell, $\delta n(0)/n_N$, for R_P^z and R_P^m as functions of the parameter α. The curves are for $n_N = 0.0185\ \text{fm}^{-3}$

for densities $n > n_u$. The radius increases with increasing density, reaches a maximum and then decreases. These results correspond to $B_N = 31.6$ MeV fm^5. The values of R_P^m practically do not depend on density. For $B_N = 31.6$ MeV fm^5 $R_P^m \cong 1.7$ fm and for $B_N = B_S$, $R_P^m \cong 1.8$ fm in the whole density range $n < n_1$ ($\alpha = 2.0$).

In Fig. 8 the energy difference ΔE_m is shown as a function of α for fixed density $n_N = 0.0185\ \text{fm}^{-3}$ and for $B_N = 31.6$ MeV fm^5. The minimum occurs at $\alpha \cong 2.5$ and ΔE_m is negative for α in the range $0.70 < \alpha < 10.0$. In Fig. 9 we display the radius R_P^m as a function of α for this particular density. The radius increases with increasing values of α reaching 3.6 fm at the highest value of α. Also the radius R_P^z is shown in this figure displaying a similar behaviour, i.e. increasing with α up to 8.5 fm at $\alpha = 7.0$. Corresponding values of the relative density excess at the center of the Wigner-Seitz cell, $\delta n(0)/n_N$, for

$R_p = R_p^m$ and $R_p = R_p^z$ are shown as functions of α in the Fig. 10. In the former case the density excess first increases for $\alpha < 2.0$ and then decreases with increasing α. In the latter case the density excess is rather constant and small after sharp decrease for $\alpha < 2.0$.

5. *Discussion of the results*

We have shown above that proton impurities in uniform density neutron matter can become localized at certain densities by suitable deformations of the neutron background. The chemical potential of the localized proton

$$\mu_P^L(n_N) = \mu_P(n_N) + \Delta E_m(n_N) \tag{33}$$

is lower than for the nonlocalized case for $n < n_l$ and $n > n_u$. At low proton concentrations x we can write the chemical potential of nonlocalized protons as

$$\mu_P(n_N, n_P) \cong \mu_P(n_N) + \frac{\partial \mu_P}{\partial n_P}(n_N) x n_N. \tag{34}$$

The last term varies as $x^{2/3}$ for small x. The chemical potential for localized protons does not depend on x for $x \ll x_c$ and

$$\mu_P^L(n_N, n_P) \cong \mu_P^L(n_N), \tag{35}$$

where $\mu_P^L(n_N)$ is given by Eq. (33). This means that for low x the configuration with localized protons is preferred energetically to the one with nonlocalized protons. At low densities, however, the state with the protons confined to the nuclei immersed in a neutron gas has still lower proton chemical potential and forms the ground state of the system [3]. Thus the state with localized single protons is a metastable one for $n < n_l$. Calculations show [3] that the nuclei disappear at a density slightly lower than the saturation density and at higher densities the uniform state with delocalized protons has lower energy. Our results show that, for low x, the state with localized single protons has lower energy than a uniform configuration for $n > n_u$. This means that in the ground state of the system for $n > n_u$ the single protons are localized.

We have assumed that the neutron background can be treated in the Thomas-Fermi approximation and the interaction of a single proton with the background is properly accounted for by a local value of the proton chemical potential. The energy difference ΔE, Eq. (30), was calculated assuming that the proton effective mass depends only on the mean neutron density n_N, Eq. (21). With this assumption we have neglected in the energy density a term proportional to $\alpha(t_1 + t_2)\Psi_P^* \Psi_P (\vec{\nabla} \Psi_P)^2$ which gives rise to a contribution to ΔE proportional to αR_P^{-5}. Such a term is a small correction to the gradient term. To account for the corresponding uncertainty we show results for two values of the gradient term parameter B_N.

In the Thomas-Fermi Hamiltonian, Eq. (22), only the lowest-order gradient term is present. This Hamiltonian is thus valid only for sufficiently slowly varying density distributions. Higher order terms will be of importance for small values of R_P which is the size of the neutron distribution inhomogeneity. One can notice that for higher values of

the parameter α we obtain slowly varying neutron distributions and the lowest order gradient term is expected to be sufficient in this case.

In view of this fact one should take the values of ΔE_m with some caution, especially those corresponding to small values of R_P. Higher order terms are expected to increase the energy E_L at low values of R_P. On the other hand they are less important at higher values of R_P and, in particular, we expect the values of R_P^z, corresponding to the onset of instability, to be rather insensitive to these corrections.

The calculations presented here are of variational nature so that the obtained energy is an upper limit to the true energy. Exact solution will lower the energy.

Another uncertainty of our conclusions is related to the Skyrme parametrization of nucleon interactions. The parameters of the Hamiltonian (8) are chosen to fit the properties of nuclei [11] and some calculations of neutron matter energy [20]. They are thus supposed to account properly for nuclear interactions at densities below the saturation density $n_0 = 0.17\,\mathrm{fm}^{-3}$. Extrapolation to higher densities is subject to uncertainty. We use thus two sets of the Skyrme parameters which give a different high density behaviour.

The nature of the phase with localized protons should be studied more carefully. In the Wigner-Seitz approximation we are not able to distinguish a solid phase and a more disordered configuration in which "dressed protons" would behave very much like a gas of nuclei in a neutron background. At very low proton concentrations one would expect the latter possibility to occur.

6. *Implications for magnetic properties of neutron matter with a small proton fraction*

The localized proton phase would have profound consequences for the magnetic properties of the neutron matter containing a small proton admixture. Localized protons in the presence of unpolarized neutron background (i.e. neglecting spin interactions) would have their magnetic moments unchanged and the system could become polarized by a residual magnetic field in the same way as the usual ferromagnets. When we account for the nuclear spin interactions which are quite strong it turns out that the neutron background is polarized and the localized proton creates a magnetic domain.

Let us assume for simplicity the effective proton-neutron spin-spin interaction to be a contact potential [21]

$$V_\sigma = g^{pn}\vec{\sigma}_1 \cdot \vec{\sigma}_2 \delta(\vec{r}_1 - \vec{r}_2). \tag{36}$$

The main contributions to the strength g^{pn} come from the one-pion exchange, the ϱ-exchange and the second-order tensor interaction [22]. The above three contributions, calculated in Ref. [22], give the value $g^{pn} \cong -2.0\,\mathrm{fm}^2$.

To see that the system is unstable with respect to small spin fluctuations we calculate the energy variation $\delta\varepsilon$ associated with a small polarization $\delta s_N(r) = n_\uparrow(r) - n_\downarrow(r)$ of the neutron background in the cell along the direction of the proton spin:

$$\delta\varepsilon = \frac{1}{2N_N}(1 + G_0^{NN})\,\delta s_N(r)^2 + g^{pn}\delta s_N \Psi_P^*(r)\Psi_P(r). \tag{37}$$

The first term is the change of the neutron energy density [2] expressed in terms of the Landau Fermi-liquid theory; G_0^{NN} is the spin-dependent Landau parameter for neutron matter; $G_0^{NN} \cong 1.0$ [23], and N_N is the neutron density of states at the Fermi level. The second term is the interaction energy due to the spin potential Eq. (36).

Minimizing the energy variation $\delta\varepsilon$ (37) with respect to $\delta s_N(r)$ we find

$$\delta s_N(r) = -\frac{g^{pn} N_N}{1+G_0^{NN}} \Psi_P^*(r)\Psi_P(r) \tag{38}$$

and the corresponding $\delta\varepsilon_{min}$

$$\delta\varepsilon_{min}(r) = -\frac{N_N}{2(1+G_0^{NN})} (g^{pn})^2 [\Psi_P^*(r)\Psi_P(r)]^2. \tag{39}$$

Integrating $\delta\varepsilon_{min}(r)$ over the whole Wigner-Seitz cell we find the energy of the cell with the polarized neutrons to be lower than the energy with unpolarized background neutrons provided there exists any proton-neutron spin interaction.

The magnetic moment of the cell, which we will call the effective magnetic moment of the proton, is

$$\mu_{eff} = \mu_P + \mu_N \int d^3r \delta s_N(r). \tag{40}$$

Here μ_P and μ_N are the proton and neutron magnetic moments, respectively, and $\delta s_N(r)$ is given by Eq. (38). The system thus behaves, in the Wigner-Seitz approximation, as a collection of magnetic domains, each of them possessing a magnetic moment μ_{eff}. Such a system displays a ferromagnetic instability as discussed above.

Magnetic phase of the strongly asymmetric nuclear matter is of importance for neutron star physics as it can produce a permanent magnetic field. Most of the neutron stars possess strong magnetic fields of the order 10^8 to 10^{12} G. This subject will be considered in detail elsewhere.

We are grateful to P. Haensel and W. Broniowski for interesting discussions on subjects considered here.

REFERENCES

[1] For a review of the neutron star matter properties we refer to: G. Baym, C. J. Pethick, *Ann. Rev. Nucl. Sci.* **25**, 27 (1975), *Ann. Rev. Astron. Astrophys.* **17**, 415 (1979).
[2] M. Kutschera, W. Wójcik, *Phys. Lett.* **223B**, 11 (1989).
[3] G. Baym, H. A. Bethe, C. J. Pethick, *Nucl. Phys.* **A175**, 225 (1971).
[4] O. Sjöberg, *Nucl. Phys.* **A265**, 511 (1976).
[5] D. Vollhardt, *Rev. Mod. Phys.* **56**, 99 (1984).
[6] T. D. Lee, *Particle Physics and Introduction to Field Theory*, Harwood Academic Publishers, New York 1981.
[7] D. Q. Lamb, J. M. Lattimer, C. J. Pethick, D. G. Ravenhall, *Phys. Rev. Lett.* **41**, 1623 (1978).
[8] J. M. Lattimer, D. G. Ravenhall, *Astrophys. J.* **223**, 314 (1978).
[9] D. Q. Lamb, J. M. Lattimer, C. J. Pethick, D. G. Ravenhall, *Nucl. Phys.* **A360**, 459 (1981).
[10] J. M. Lattimer, *Ann. Rev. Nucl. Part. Sci.* **31**, 337 (1981).

[11] D. Vautherin, D. M. Brink, *Phys. Lett.* **32B**, 149 (1970).
[12] D. G. Ravenhall, C. D. Bennet, C. J. Pethick, *Phys. Rev. Lett.* **28**, 978 (1972).
[13] T. H. R. Skyrme, *Nucl. Phys.* **9**, 615 (1959).
[14] H. A. Bethe, *Phys. Rev.* **167**, 879 (1968).
[15] H. A. Bethe, *Ann. Rev. Nucl. Sci.* **21**, 93 (1971).
[16] Z. Barkat, J. R. Buchler, L. Ingber, *Astrophys. J.* **176**, 723 (1972).
[17] R. J. Lombard, *Ann. Phys.* (*N.Y.*) **77**, 380 (1973).
[18] K. A. Brueckner, J. R. Buchler, R. Clark, R. J. Lombard, *Phys. Rev.* **181**, 1543 (1969).
[19] K. A. Brueckner, J. R. Buchler, S. Jorna, R. J. Lombard, *Phys. Rev.* **171**, 1188 (1969).
[20] P. J. Siemens, V. R. Pandharipande, *Nucl. Phys.* **A173**, 561 (1971).
[21] G. E. Brown, S. O. Bäckman, E. Oset, W. Weise, *Nucl. Phys.* **A286**, 191 (1977).
[22] S. O. Bäckman, G. E. Brown, J. A. Niskanen, *Phys. Rep.* **124**, 1 (1985).
[23] S. O. Bäckman, C. G. Källman, O. Sjöberg, *Phys. Lett.* **43B**, 263 (1973).